JVI Journals.ASM.org

Oncogenic Human T-Cell Lymphotropic Virus Type 1 Tax Suppression of Primary Innate Immune Signaling Pathways

Jinhee Hyun,[a] Juan Carlos Ramos,[b] Ngoc Toomey,[b] Siddharth Balachandran,[c] Alfonso Lavorgna,[d] Edward Harhaj,[d] Glen N. Barber[a]

Department of Cell Biology[a] and Department of Medicine,[b] Sylvester Comprehensive Cancer Center, University of Miami Miller School of Medicine, Miami, Florida, USA; Fox Chase Cancer Center, Philadelphia, Pennsylvania, USA[c]; Department of Oncology, Johns Hopkins School of Medicine, Baltimore, Maryland, USA[d]

ABSTRACT

Human T-cell lymphotropic virus type I (HTLV-1) is an oncogenic retrovirus considered to be the etiological agent of adult T-cell leukemia (ATL). The viral transactivator Tax is regarded as the oncoprotein responsible for contributing toward the transformation process. Here, we demonstrate that Tax potently inhibits the activity of DEx(D/H) box helicases RIG-I and MDA5 as well as Toll-dependent TIR-domain-containing adapter-inducing interferon-β (TRIF), which function as cellular sensors or mediators of viral RNA and facilitate innate immune responses, including the production of type I IFN. Tax manifested this function by binding to the RIP homotypic interaction motif (RHIM) domains of TRIF and RIP1 to disrupt interferon regulatory factor 7 (IRF7) activity, a critical type I IFN transcription factor. These data provide further mechanistic insight into HTLV-1-mediated subversion of cellular host defense responses, which may help explain HTLV-1-related pathogenesis and oncogenesis.

IMPORTANCE

It is predicted that up to 15% of all human cancers may involve virus infection. For example, human T-cell lymphotropic virus type 1 (HTLV-1) has been reported to infect up to 25 million people worldwide and is the causative agent of adult T-cell leukemia (ATL). We show here that HTLV-1 may be able to successfully infect the T cells and remain latent due to the virally encoded product Tax inhibiting a key host defense pathway. Understanding the mechanisms by which Tax subverts the immune system may lead to the development of a therapeutic treatment for HTLV-1-mediated disease.

The vertebrate innate immune system is critical for the early detection and control of infection by microorganisms. Recognition of an infection proceeds via detection of the infectious agent by pattern recognition receptors (PRRs), an important class of which are the Toll-like receptors (TLRs) (1, 2). TLRs recognize pathogen-associated molecular patterns (PAMPs), such as single- and double-stranded RNA (ssRNA and dsRNA), via their extracellular leucine-rich region (LRR) and activate signaling cascades through a cytoplasmic Toll/interleukin-1β (IL-1β) homology (TIR) domain that culminates, through using intermediate molecules such as MyD88, TNF receptor-associated factor 3 (TRAF3), and/or TIR domain-containing adapter-inducing interferon-β (TRIF), in the activation of NF-κB- and interferon regulatory factor 3/7 (IRF3/7)-dependent antimicrobial gene expression, including type I interferon (IFN). For example, TLR3 is an interferon-inducible TLR expressed in a wide variety of tissues that can recognize viral dsRNA species and trigger TRIF-dependent transcriptional activation of type I IFN (3–6). In contrast, TLR7 and TLR8 are specific to plasmacytoid dendritic cells (pDCs) and can potently induce IFN production following recognition of viral single-stranded species via MyD88/TRIF-dependent signaling (7–9).

Recently, the caspase recruitment domain (CARD)-containing DEx(D/H) box helicases RIG-I and MDA5 have emerged as critical, TLR-independent detectors of viral infection (10–12). These helicases are activated by cytosolic RNA intermediates produced during viral replication. Mitochondrial IPS-1 (also called MAVS, VISA, or Cardif) has been shown to be essential for RIG-I- and MDA5-mediated establishment of an antiviral state (13–16). While the molecular mechanisms underlying IPS-1-mediated activation remain to be fully clarified, evidence indicates important downstream roles for Fas-associated protein with death domain (FADD), receptor-interacting protein 1 (RIP1), TRAF3, and NF-κB essential modifier (NEMO) (also known as IκB kinase gamma [IKK-γ]) in similarly activating NF-κB- and IRF-3/7-dependent IFN induction (17–19). The importance of these pathways in mediating effective host defense is emphasized by the growing number of virus types that have evolved ways to suppress the function of these molecules.

HTLV-1 is the prototypic deltaretrovirus, a subgroup of *Retroviridae* (20). Infection of T lymphocytes by HTLV-1 can result in adult T cell leukemia (ATL), a severe, fatal lymphoma (21, 22). In addition to ATL, HTLV-1 has also been implicated in a tropical spastic paraparesis/HTLV-1-associated myelopathy (TSP/HAM), a neurodegenerative disorder (23). Approximately 1 to 3% of HTLV-1-infected individuals develop ATL or TSP/HAM following a lengthy period of viral persistence (24). The Tax protein encoded by HTLV-1 is thought to be the crucial mediator of malignant T cell transformation by HTLV-1 and is independently capable of transforming both rodent fibroblasts and human T lymphocytes (25–28). Although primarily a nuclear protein, a proportion of Tax localizes to the cytoplasm and exerts its growth-

Received 29 August 2014 **Accepted** 6 February 2015

Accepted manuscript posted online 18 February 2015

Citation Hyun J, Ramos JC, Toomey N, Balachandran S, Lavorgna A, Harhaj E, Barber GN. 2015. Oncogenic human T-cell lymphotropic virus type 1 Tax suppression of primary innate immune signaling pathways. J Virol 89:4880–4893. doi:10.1128/JVI.02493-14.

Editor: S. R. Ross

Address correspondence to Glen N. Barber, gbarber@med.miami.edu.

doi:10.1128/JVI.02493-14

promoting properties by engaging a wide variety of signaling cascades (29). For example, via stimulation of CREB, NF-κB, and serum response factor (SRF) transcription factors, Tax can transactivate a diverse array of cellular genes, including those encoding proliferative cytokines, cytokine receptors, costimulatory molecules, and cell survival proteins (30–32). In addition to its ability to modulate cellular gene expression at the transcriptional level, Tax can also interfere with the cell cycle and promote cell growth by direct interactions with, for example, cyclin-dependent kinase complexes and centrosomal components (33, 34).

During a screen for virally encoded regulators of host defense, we observed that HTLV-1 Tax could potently inhibit innate immune signaling events triggered by dsRNA. This included the inhibition of TRIF-dependent TLR pathways, as well as RIG-I/MDA5-dependent TLR-independent pathways and the recently discovered STING pathway essential for DNA-mediated innate signaling (35, 36). Tax achieved this by preventing effective IRF7 function required for the transcriptional induction of type I IFNs as well as other innate immune genes. However, NF-κB pathways were not suppressed and essentially exhibited greater activity in the presence of Tax. ATL cells exhibited defects in innate signaling function and, as such, were sensitive to vesicular stomatitis virus (VSV)-mediated oncolysis. Our data demonstrate that in addition to its well-described roles in cell survival and cell growth control, Tax can also modulate the host innate immune response to favor virus replication and oncogenesis.

MATERIALS AND METHODS

Cells, recombinant virus, reagents, and antibodies. HeLa cells, 293T cells, BHK cells, and mouse embryonic fibroblasts (MEFs) were grown in Dulbecco's modified Eagle medium (DMEM) supplemented with 10% fetal bovine serum (FBS) and antibiotics. Jurkat Tet-on Tax, Jurkat E6.1, and primary ATL cells were grown in RPMI 1640 medium with 10% FBS, 2 mM glutamine, and antibiotics. Strain Indiana of VSV-GFP (green fluorescent protein) and VSVΔM were previously generated in our lab. Poly(I·C) (1 μg/ml) was purchased from Invivogen. Doxycycline (1 μg/ml), G418, and Polybrene were obtained from Sigma. The QuikChange site-directed mutagenesis kit was from Stratagene. Murine IFN-α and IFN-β enzyme-linked immunosorbent assay (ELISA) kits were acquired from PBL. Polyclonal VSV antiserum was produced from BALB/c mice after they were immunized against wild-type VSV. Monoclonal anti-Tax antibody was a gift from E. Harhaj. Other antibodies used in this study were FLAG (Sigma), IRF3, IRF7, and Myc (Santa Cruz Biotechnology), pIRF7 and hemagglutinin (HA) (Cell Signaling), TBK1 (Abcam), and RIP1 (BD Science, Abcam).

Transfections and viral infections. Transfections were done using Lipofectamine 2000 (Invitrogen) in Opti-MeM, a serum-free medium (Invitrogen) according to the manufacturer's manual. MEF transfection was carried out using the Amaxa MEF Nucleofectin kit 1 according to the manufacturer's recommendations (Amaxa Biosystems). Jurkat transfections were performed with Fugene HD (Roche) as described by the manufacturer.

Viral infection and titer analysis were performed as described previously. Briefly, 70% of confluence cell cultures were infected with recombinant virus at the indicated multiplicity of infection (MOI) with serum-free medium. After 1 h of incubation, the plates were rinsed with phosphate-buffered saline (PBS) twice and replenished with complete medium. BHK cells were employed for VSV-GFP viral titers.

Plasmids and mutagenesis. Expression vectors FLAG, GFP, and HA-tagged human RIG-I, MDA-5, ΔRIG-I, ΔMDA5, IPS1, TBK1, and RIP1 were previously generated in G. N. Barber's lab. FLAG-RIP1 variants were created by PCR (Invitrogen) using the EcoR I/HindIII enzyme site and site-directed mutagenesis kit (Stratagene). The following oligonucleotides were used for construction of RIP1 mutants: CTCATGATCATGGCGAC AGTGTACAAGGG and CCCTTGTACACTGTCGCCATGATCATGAG for K45A, CCGAATTCACCATGGACTACAAGGACGACGACGATAA GATGCAACCAGACATGTCCTT and GGAAGCTTTTAAGGTGTTTA TCCGTCA for KD-ID, CCGAATTCACCATGGACTACAAGGACGACG ACGATAAGATGCAACCAGACATGTCCTT and GGAAGCTTTTAGT CCTCTTCTACACTTTCTT for KD, CCGAATTCACCATGGACTACAA GGACGACGACGATAAGGTGAAGAGTTTAAAGAAAGA and GGAA GCTTTTAAGGTGTTT ATCCGTCA for ID, CCGAATTCACCAT GGACTACAAGGACGACGACGATAAGGTTGTGAAGAGAATGC AGTC and GGAAGCTTTTAGTTCTGGCTGACGTAAATC for ID-DD, CCGAATTCACCATGGACTACAAGGACGACGACGATAAGCCAATC AGGGAAAATCTGGG and GGAAGCTTTTAGTTCTGGCTGACGTA AATC for DD, CCGAATTCACCATGGACTACAAGGACGACGACGAT AAGTCAATTAGAAGAAAGTGTAG and GGAAGCTTTTATATGACT TGGAATTGGCCTG for ID12, CCGAA TTCACCATGGACTACAAGG ACGACGACGATAAGGGACAGGCAGACGAAACAGC and GGAA GCTT TTAGTCCTCTTCT ACACTTTCTT for ID 23, TATGGCAGCC GCATAGGCCAATTCCAAG and CTTGGAATTGGCCTATGCGGCTG CCATA for dID2. The following other plasmids were obtained from the sources shown in parentheses: HTLV Tax, Gal4-Luc, Gal4-IRF3, and Gal4-IRF7 (E. Harhaj), FLAG-TRAF3, HA-TRAF3, and FLAG-TANK (G. Cheng), Myc-IRF7 and Myc-RIP1(S. Ning), FLAG-IRF3, FLAG-IRF7, and IFN-β Luc (J. Hiscott), PRD II Luc and PRD-III-I Luc (T. Maniatis), and IRF3 (superactive mutant) and IRF7 (superactive mutant) (Invivogen).

Real-time PCR. Total RNA was isolated using the RNeasy RNA extraction kit (Qiagen), and cDNA synthesis (Invitrogen) was performed with random primers using 1 μg of total RNA. Real-time PCR was performed using a LightCycler 2.0 instrument and the TaqMan Gene Expression assay (Life Technologies). TaqMan probes mIFNb (Mm00439546) and hIFNhb (Hs00185375) were used for experiments. Each sample was normalized to internal control 18S rRNA.

Reporter gene assays and coimmunoprecipitations. For reporter gene assays, 293T cells were placed in 24-well plates and transiently transfected with 50 ng of luciferase reporter plasmid, 10 ng of pRL-TK, and 100 to 200 ng of expression plasmids by using Lipofectamine 2000 (Invitrogen). For Jurkat cells, 500 ng of reporter plasmid, 100 ng of pRL-TK, and 1 μg of expression plasmid were used in the experiments. After 24 or 36 h, the cells were ruptured with cell culture lysis buffer (Promega) and luciferase activity was measured using a luminometer (TD 20/20; Turner Designs). All luciferase assay results were presented as fold induction values.

For coimmunoprecipitations, expression vectors were transfected into 293T cells for 36 h, cells were lysed in EBC10 (50 mM Tris [pH 8.0], 150 mM NaCl, 0.1% NP-40, 50 mM NaF, 1 mM Na_3VO_4, 1 mM dithiothreitol [DTT]) or radioimmunoprecipitation assay (RIPA) buffer (Pierce) with protease inhibitors (100 mM phenylmethylsulfonyl fluoride [PMSF], leupeptin, aprotinin, pepstatin). Lysates (1 mg) were precipitated with 1 μg of FLAG monoclonal antibody (MAb; Sigma) overnight at 4°C. All precipitates were washed with lysis buffer 5 times, and proteins were released by 2× sample buffer after boiling and analyzed by SDS-PAGE.

Immunofluorescence and ELISAs. Jurkat T cell or primary ATL cells were seeded on glass coverslips coated with poly-L-lysine in 12-well plates and centrifuged at 2,000 × *g* for 5 min. Cells were washed with PBS and fixed with 1% paraformaldehyde for 10 min. After permeabilizing cells with 0.2% Triton X-100 for 10 min, the cells were blocked in PBS containing 10% serum for 1 h and stained with anti-Tax or other indicated antibodies for 1 h. The cells were washed with PBS 3 times. Secondary antibodies Alexa-Fluor 555-conjugated donkey anti-mouse IgG and Alexa Fluor 488-conjugated donkey anti-rabbit IgG (Life Technologies) were used at 1:500 to 1:1,000 dilution. Nuclei were stained with 4′,6-diamidino-2-phenylindole (DAPI; Invitrogen). Finally, samples were mounted using ProLong gold antifade reagents (Invitrogen).

Supernatants from 293T cells were transfected with expression plas-

mids encoding HTLV-1 Tax and the active form of RIG-I (amino acids [aa] 1 to 284). To determine the secreted IFN amounts, ELISAs were performed according to the manufacturer's instructions (PBL Interferon Source).

Native PAGE gel. Native PAGE gel analysis was carried out after 293T cells were transfected with the indicated plasmids or treated with poly(I·C) for 6 h and cells were lysed with native lysis buffer (50 mM Tris-Cl [pH 8.0], 1% NP-40, 150 mM NaCl, 100 mg/ml leupeptin, 1 mM PMSF, 5 mM orthovanadate). The lysates were subjected to nondenaturing electrophoresis.

Yeast two-hybrid analysis. The Matchmaker yeast two-hybrid system 3 (BD Biosciences Clontech, CA) was used for two-hybrid assays. Full-length HTLV-1 Tax or human RIP1 was inserted into pGBK7 (bait vector), and other genes encoding FADD, IPS, RIG-I variants, and MDA-5 variants were cloned into pGADT7 vector. A molar ratio of 2:1 of pGBKT7 and pGADT7 (Clontech) was used for cotransformations in *Saccharomyces cerevisiae* strain AH109. The transformed colonies were plated on synthetic defined (SD)-Trp plates for pGBKT7 selection or SD/-Leu/-Trp plates for cotransformed yeast clones containing pGBKT7 (DNA bait) and pGADT7 (AD/library) plasmids. After several days of incubation at 30°C, several single colonies from cotransformed clones were "patched" onto SD/-Leu/-Trp plates and following sufficient growth (1 to 2 days) were streaked onto SD/-Leu/-Trp (low-stringency plates), SD/-His/-Leu/-Trp (medium-stringency plates), and SD/-Ade/-His/-Leu/-Trp (high-stringency plates) to investigate any potential interaction between the viral "bait" and the library/host protein.

Poly(I·C)-agarose precipitation. To determine whether endogenous RIG-I, MDA-5, RIP1, FADD, or PKR interacted with poly(I·C)-agarose, HeLa cells (1×10^7 per condition) either were left untreated or were treated with hIFN-β (100 U/ml) for 18 h and with poly(I·C) for a further 3 h. Cells were then lysed in B II (20 mM Tris-HCl [pH 7.4], 150 mM NaCl, 0.2% Nonidet P-40, 8% glycerol, and protease inhibitors). Lysates were precleared by brief sonication, centrifugation, and incubation with agarose beads for 1 h. They were then incubated with poly(I·C)-agarose (Amersham) for 4 h, washed extensively with cold lysis buffer II, resolved by SDS-PAGE, and detected by standard immunoblotting using the indicated antibodies.

RESULTS

Tax inhibits induction of type I IFN by poly(I·C). An evaluation of HTLV-1 Tax's effects on intracellular signaling indicated that Tax could potently inhibit the ability of dsRNA to trigger activation of the IFN-β promoter in HeLa cells (Fig. 1A). Previous data have indicated that RIG-I and MDA5 are key cellular sensors responsible for recognizing viral RNA species and for invoking the production of type I IFN (10, 37). To extend this analysis, we cotransfected 293T cells with expression vectors encoding either full-length RIG-I or MDA-5, together with increasing amounts Tax. Such cells were subsequently transfected with dsRNA and assayed for IFN-β promoter induction. This study indicated that cells overexpressing Tax displayed a significant dose-dependent impairment in dsRNA-induced RIG-I- or MDA-5-mediated activation of the IFN-β promoter (~80% reduction) (Fig. 1B). It has also been demonstrated that the CARDs of RIG-I and MDA-5 alone have been shown to constitutively activate the IFN-β gene in the absence of poly(I·C) or viral stimulation (10, 13). Accordingly, we observed that Tax was also able to potently inhibit type I IFN-dependent signaling and IFN-β protein production mediated by the CARDs of RIG-I and MDA-5 alone (Fig. 1C and D). Similar effects were observed in Tax-expressing Jurkat T cells (Fig. 1E). This analysis would indicate that HTLV-1 Tax inhibits the production of type I IFN by preventing the downstream function of the CARDs of RIG-I and MDA5.

The inhibition of innate immune responses has been shown to render nontransformed cells permissive to virus infection (38). Thus, we next evaluated whether Tax expression could increase the permissiveness of murine embryonic fibroblasts (MEFs) to vesicular stomatitis virus (VSV) infection, a virus known to be sensitive to the antiviral effect of IFN (39). Primary C57BL/6 MEFs overexpressing Tax or control cells transfected with an empty vector were next infected with different multiplicities of infection (MOIs) of recombinant VSV expressing GFP. These experiments indicated that infected MEFs overexpressing Tax exhibited significantly greater cytolysis and GFP fluorescence than control cells (Fig. 1F). In agreement with these observations, we noticed that approximately 10-fold more progeny virus was recovered from the supernatants of infected MEFs overexpressing Tax (Fig. 1G). Overexpressed Tax in primary C57BL/6 MEFs also inhibited endogenous *ifnb* gene transcription in response to poly(I·C) (Fig. 1H). To what extent Tax could inhibit the induction of type I IFN was further evaluated using Tax-inducible T cell lines (Jurkat). Following Dox withdrawal, Tax expression was seen to increase as deduced by immunofluorescence and immunoblot analysis (Fig. 1I; expression is shown in red). To confirm that Tax impedes the induction of type I IFN, we infected T cells, Tax induced or noninduced, with a VSV mutant virus (VSVΔM) defective in viral matrix (M) activity (an alanine substitution at position 51, which is unable to prevent host IFN mRNA export and translation) (40). This analysis indicated a decrease in VSVΔM-induced IFN-β mRNA production in the presence of Tax (2- to 5-fold; Fig. 1J). Finally, HTLV-1-infected human cells in which Tax was expressed at high levels (MT-4) did not robustly respond to type I IFN induction following transfection with poly(I·C). This was in contrast to cells that expressed low levels of Tax (ATLL-84c), which remained able to trigger type I IFN production following stimulation of the RIG-I/MDA5 pathway (Fig. 1K). Taken together, these results demonstrate that Tax can inhibit RIG-I- and MDA-5-triggered type I IFN signaling and render cells susceptible to virus infection.

Tax inhibits RIG-I-activated IRF3/7, but not NF-κB, signaling. We next evaluated where in the RIG-I pathway Tax exerted its suppressive influence. Our experiments indicated that Tax could inhibit the activation of the IFN-β promoter by IPS-1, as well as RIG-I/MDA5 (Fig. 2A). However, Tax could not inhibit heterologously expressed TBK-1 or constitutively active IRF3 (SA) or IRF7 (SA), suggesting that Tax's inhibitory effects were upstream of IRF3/7. RIG-I-and MDA-5-dependent antiviral gene expression has been shown to require the coordinated activation of both the IRF3/7 and the NF-κB classes of transcription factors (41). Therefore, we next evaluated the effect of Tax on specific activation of either IRF3/7 (PRD III-I)- or NF-κB (PRD II)-dependent elements from the human *ifnb* gene by the CARDs of RIG-I and MDA-5. These experiments indicated that Tax was able to potently inhibit RIG-I CARD- and MDA-5 CARD-dependent activation of PRD III-I in a dose-dependent manner (Fig. 2B). In contrast to its effect on IRF3/7-dependent signaling, and in agreement with previous reports, we found that Tax alone potently activated NF-κB-dependent signaling, as measured by stimulation of the PRD II-Luc reporter plasmid (Fig. 2C). These results suggest that Tax can selectively inhibit IRF3/7-dependent antiviral signaling mediated by RIG-I and MDA-5.

Tax interacts with RIP1. Our results and those of others suggest that RIP1 and FADD are essential downstream components

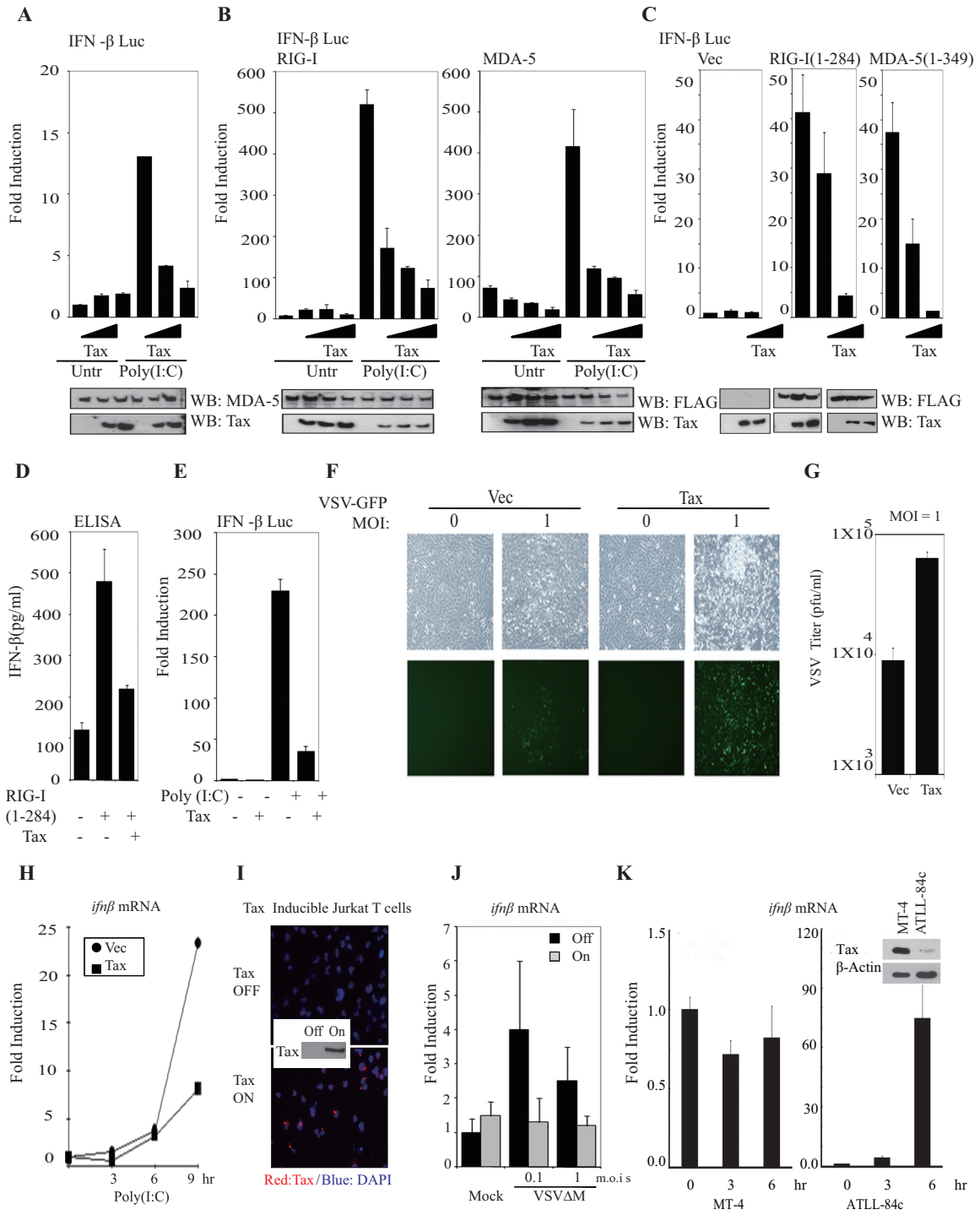

FIG 1 HTLV-1 Tax inhibits RIG-I and MDA-5 signaling. (A) An IFN-β-Luc reporter plasmid was transfected in HeLa cells with or without increasing amounts of an expression vector encoding Tax for 24 h. The cells were transfected with poly(I·C) (5 mg/ml), and luciferase activity was measured. The expression of endogenous MDA-5 and ectopic Tax were detected by immunoblotting (IB) analysis. (B) IFN-β-Luc reporter plasmids were transfected in 293T cells with expression vectors encoding either FLAG-RIG-I or FLAG-MDA-5 and with empty vector or Tax. Cells were then treated as described for panel A. (C) Luciferase reporter assays were performed in 293T cells as described for panel B using FLAG-RIG-I variants (aa 1 to 284) or FLAG-MDA-5 variants (aa 1 to 349), and increasing amounts of Tax. (D) ELISAs were performed to detect production of endogenous IFN-β protein in 293T cells after transfecting with FLAG-RIG-I (1-284) and Tax. (E) Luciferase reporter assays were performed in Jurkat T cells after transfecting IFN-β-luc, Tax, and poly(I·C) (5 mg/ml). (F) Viral replication of VSV-GFP was detected in primary C57BL/6 MEFs after transfecting with either an empty vector or Tax for 24 h. Photomicrographs were taken 24 h postinfection. (G) Standard plaque assays for viral progeny output were performed from the supernatants from cells treated as described for panel F. (H) Real-time PCR analysis of *ifn*β mRNA level in primary C57BL/6 MEFs that were transfected with either an empty control vector or Tax for 24 h and treated with poly(I·C) for the indicated periods. (I) Immunofluorescence (IF) assays were used to detect expression of Tax (red) in Tax-inducible Jurkat T cells after treating with doxycycline (1 μg/ml) for 24 h. (J) Real-time PCR analysis for *ifn*β mRNA transcription in Tax-inducible Jurkat T cells after the infection of VSVΔM for 6 h. (K) Real-time PCR analysis was performed to evaluate mRNA levels of *ifn*β in MT-4 cells or ATLL-84c cells that were treated with VSVΔM (MOIs = 1) for the indicated times. Tax expression was also tested in those cell lines by immunoblotting using anti-Tax antibody. Error bars indicate ± standard deviations (SD).

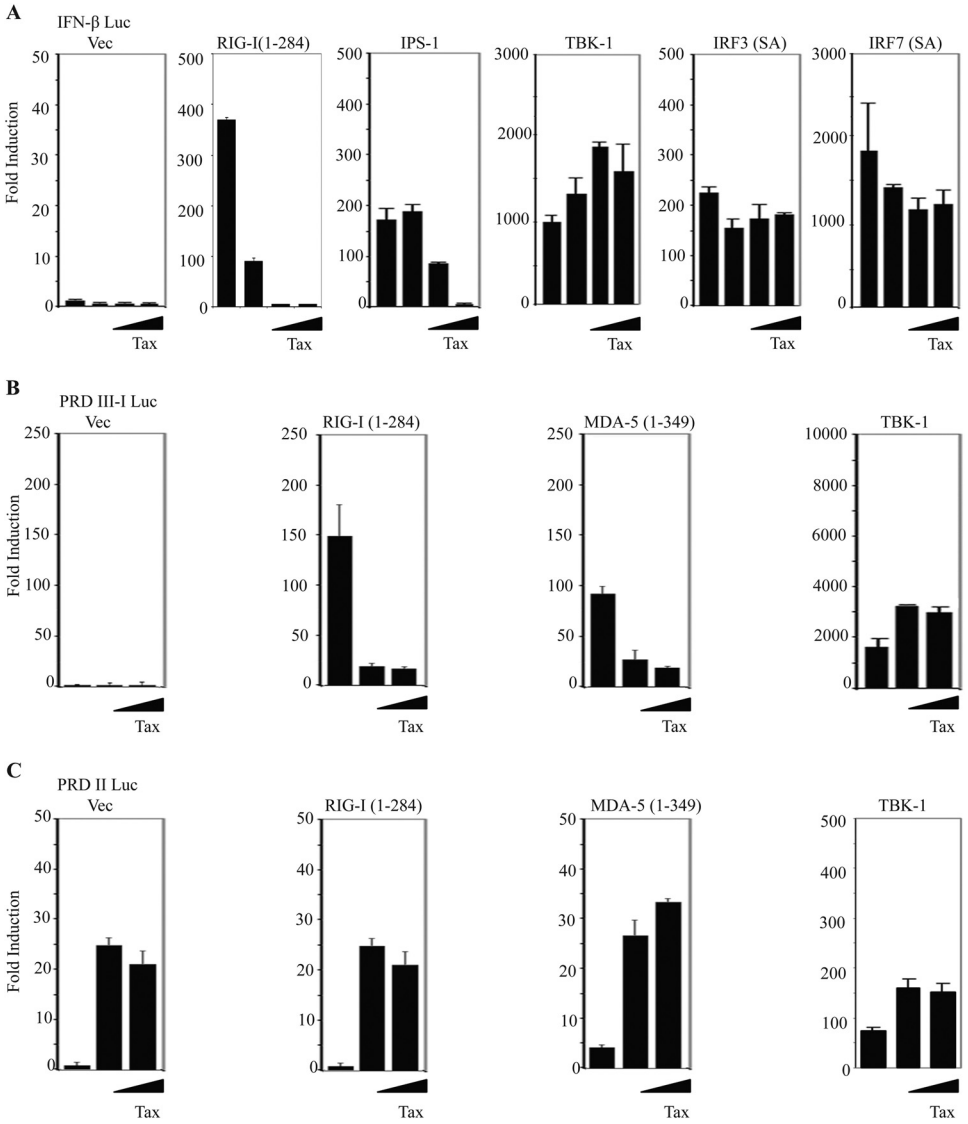

FIG 2 HTLV-1 Tax selectively inhibits IRF3/7 signaling. (A) Luciferase reporter assays were performed in 293T cells with IFN-β-luc, FLAG-RIG-I(1-284), full-length IPS-1, TRIF, TBK1, IRF3 (superactive mutant), or IRF7 (superactive mutant), with increasing amounts of Tax. (B) Luciferase reporter assays were performed in 293T cells after transfecting IRF3/7-responsive PRDIII-I-luciferase plasmid, expression vectors encoding either FLAG-RIG-I(1-284), FLAG-MDA-5(1-349), or full-length TBK1, and increasing amounts of Tax. (C) The luciferase reporter assays illustrated in panel B were performed in 293T cells with NF-κB-responsive PRDII-luciferase plasmid. Error bars, ±SD.

required by RIG-I and MDA-5 to trigger type I IFN production (17, 42–44). In an effort to obtain mechanistic insight into the ability of Tax to inhibit RIG-I- and MDA-5-dependent signaling, we performed protein binding experiments to identify potential interactions between Tax and RIG-I and MDA-5 and/or FADD and RIP1. Principally, yeast two-hybrid experiments revealed a robust and specific interaction between RIP1 and Tax but not with RIG-I/MDA5 and Tax (Fig. 3A). To determine the domains of RIP1 involved in interactions with Tax, we performed coimmunoprecipitation experiments with Tax and a variety of RIP1 variants as depicted in Fig. 3B. This analysis indicated that an intermediate domain (ID) including the RIP homotypic interaction motif (RHIM; amino acids [aa] 301 to 558) of RIP1, previously described as being essential for RIP3 interaction, was necessary and sufficient for its interaction with Tax (Fig. 3B and C) (45–47). Confocal analysis also indicated that RIP1 could colocalize with Tax in Jurkat Tax-inducible and in primary ATL cells (Fig. 3D). Of interest is that a RHIM domain has recently been found in the TLR pathway adaptor protein TRIF (also referred to as TICAM) (46, 48, 49). TRIF facilitates TLR3 and -4 activation of innate signaling processes by dsRNA and lipopolysaccharide (LPS), respectively. TRIF partially achieves this by utilizing RIP1 through RHIM association to regulate NF-κB and IRF3/7 activity. We thus evaluated the effects of Tax on TRIF function and found that Tax was able to inhibit IRF3/7-dependent PRDIII-I promoter activation by TRIF but not NF-κB signaling (Fig. 3E). Coimmunoprecipitation experiments subsequently confirmed that Tax could indeed bind to TRIF (Fig. 3F). Thus, Tax binds to regions within the RHIM domains and prevents TLR-dependent and -independent IRF3/7 but not NF-κB signaling.

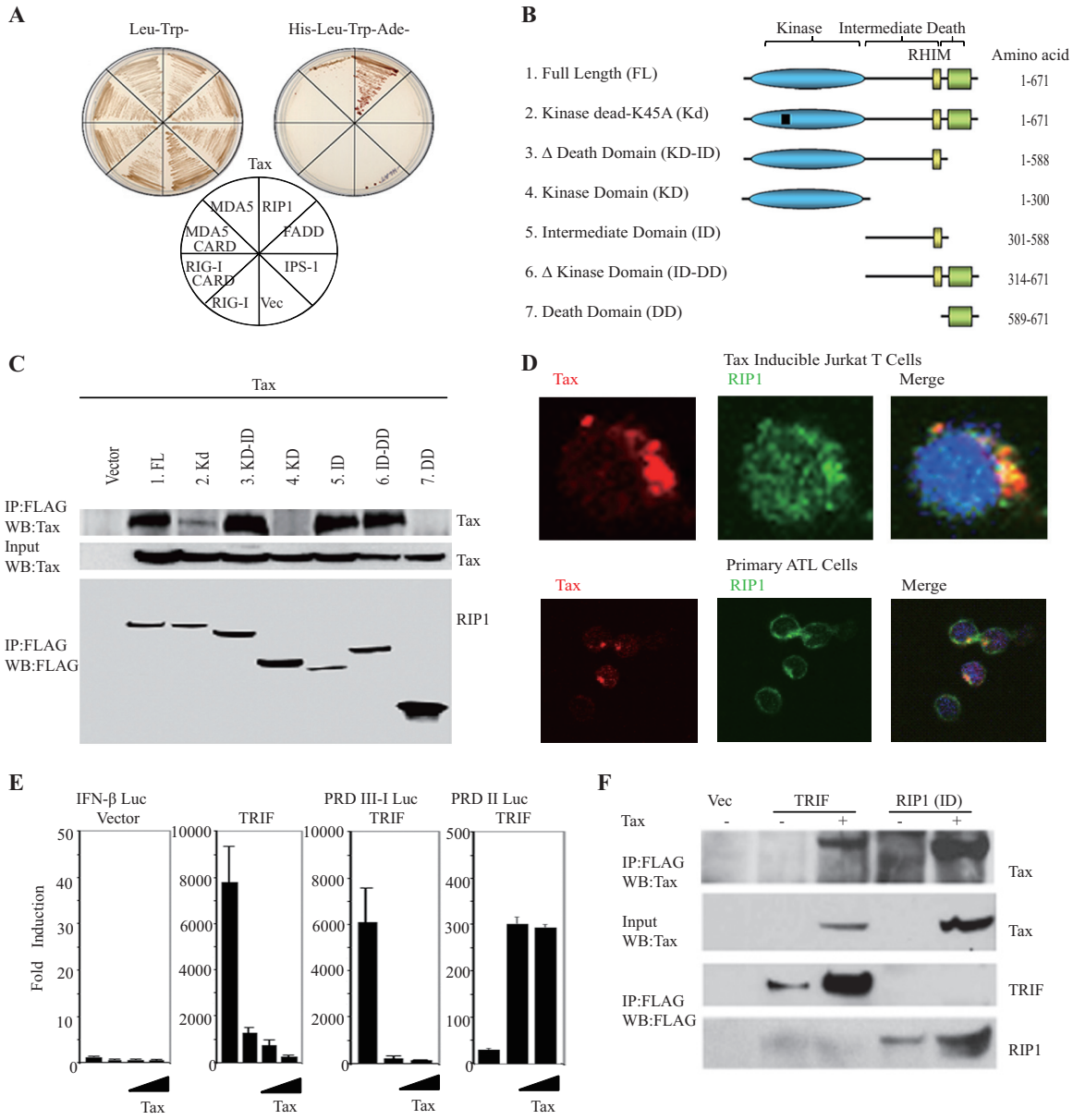

FIG 3 HTLV-1 Tax interacts with RIP1. (A) *S. cerevisiae* strain AH109 was cotransformed with Tax, together with the indicated prey plasmids. Only cells coexpressing Tax and RIP1 grew under high-stringency selection conditions, indicating interaction. (B) Schematic diagram of RIP1 and RIP1 deletion mutants. (C) Coimmunoprecipitation (Co-IP) analyses were performed in 293T cells after cotransfecting Tax and FLAG-tagged RIP1 mutants using anti-FLAG antibody. IB analysis detected the indicated proteins. (D) IF assays detected expression of Tax (red) and RIP1(green) in Tax-inducible Jurkat T cells or primary ATL cells after treating with doxycycline (1 μg/ml) for 24 h. (E) Luciferase reporter assays were performed in 293T cells after transfecting IFN-β-luc, PRD-III luciferase, or PRD-II luciferase reporter plasmids, expression vectors encoding FLAG-TRIF, and increasing amounts of Tax. (F) Co-IP analyses were performed in 293T cells after cotransfecting expression plasmids encoding Tax and the FLAG-TRIF or FLAG-RIP1 variant (aa 301 to 588). After 36 h, the cell lysates were pulled down using anti-FLAG antibody and IB analysis was performed using anti-Tax antibody. Error bars, ±SD.

RIP RHIM association with Tax and RIG-I. Our findings that Tax potently inhibits RIG-I/MDA-5- and TRIF-activated signaling prompted us to examine in greater detail the mechanistic consequences of this association. As a start to these studies, we treated HeLa cells with or without IFN-β and subjected lysates to dsRNA affinity chromatography. These experiments verified that both endogenous RIG-I and MDA-5 were able to associate with dsRNA (Fig. 4A). The interactions were more evident when endogenous RIG-I or MDA-5 was precipitated from IFN-treated cells, since these molecules are themselves IFN-inducible proteins. Interestingly, we observed that RIP1 could be precipitated by poly(I·C)-agarose in a manner that was enhanced by previous IFN treatment, suggesting that RIP1 could bind poly(I·C) directly or was being recruited to an IFN-stimulated dsRNA-dependent complex by molecules such as RIG-I and MDA-5 (Fig. 4A). However, RIP1 possesses no discernible RNA-interacting motifs and did not associate with dsRNA when produced alone in rabbit reticulocyte lysates (data not shown). To extend these studies, we transfected

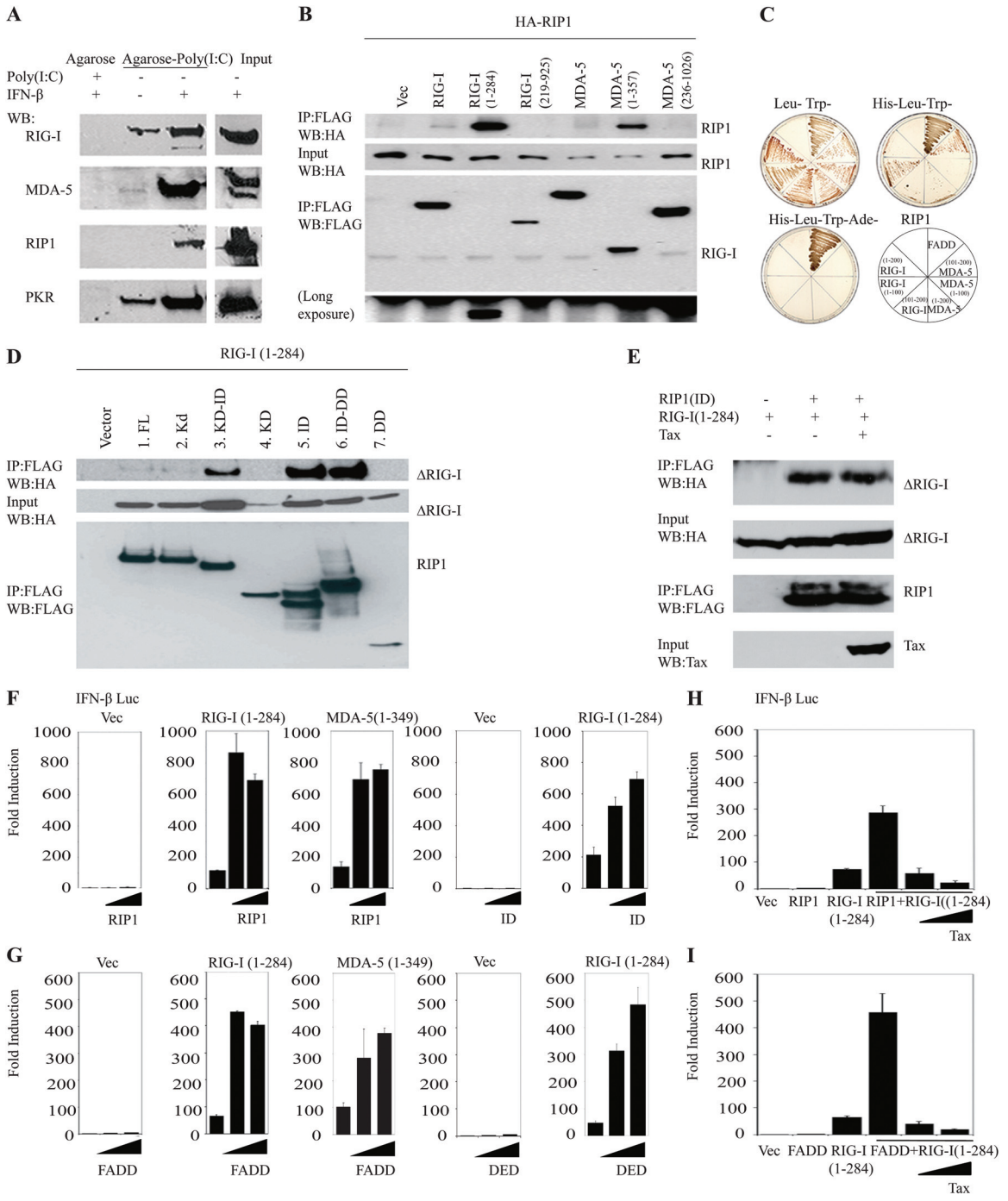

FIG 4 RIP1 associates with RIG-I in the presence of dsRNA. (A) HeLa cells were treated with or without IFN-β for 18 h and poly(I·C) for 3 h, and the lysates were subjected to poly(I·C) to dsRNA affinity chromatography. Precipitated poly(I·C) agarose was resolved by SDS electrophoresis analysis. Indicated antibodies were used for IB. (B) Co-IP analyses were performed in 293T cells transfected with HA-RIP1, either FLAG-RIG-I variants (full length, aa 1 to 284, or aa 219 to 925) or FLAG-MDA5 variants (full length, aa 1 to 357, or aa 236 to 1026). The lysates were immunoprecipitated (IP) with anti-FLAG antibody, and immunoblot analysis was performed with anti-HA antibody. (C) Yeast two-hybrid assays were used to detect the GAL4 binding domain (BD)-conjugated full-length RIP1, which strongly interacts with full-length FADD in yeast. Weak interaction of RIP1 and RIG-I (aa 1-200) or MDA-5 (aa 101-200) was also detected in the yeast two-hybrid system. The GAL4 activation domain was fused to full-length FADD, RIG-I variants (top left, aa 1-200; top right, aa 1-100; bottom left, aa 101-200), and MDA-5 variants (top left, aa 1-200; top right, 1-100; bottom left, aa 101-200). (D) Co-IP analyses were performed in 293T cells after overexpressing plasmids encoding HA-RIG-I (aa 1 to 284) and FLAG-RIP1 deletion variants. The lysates were immunoprecipitated with-anti FLAG antibody and IB analysis was performed with anti-HA antibody. (E) 293T cells were transfected with HA-RIG-I(1-284) and the FLAG-intermediate domain of RIP1(301-588), either with or without the expression vector encoding Tax. The cell lysates were immunoprecipitated, and IB analysis was performed with the indicated antibodies. (F) Luciferase reporter assays were performed in 293T cells after transfecting IFN-β-luc expression vectors, plasmids encoding either FLAG-RIG-I(1-284) or FLAG-MDA-5(1-357), and increasing amounts of an expression vector encoding full-length RIP1 or an intermediate domain of RIP1(301-588) for 36 h. (G) Luciferase reporter assays were performed in 293T cells after transfecting IFN-β-luciferase expression vectors, plasmids encoding either FLAG-RIG-I(1-284) or FLAG-MDA-5(1-357), and increasing amounts of plasmid encoding FADD or the death effector domain of FADD (aa 1 to 97) for 36 h. (H, I) IFN-β-Luciferase reporter plasmids were transfected in 293T cells with expression vectors encoding either RIG-I(1-284) along with expression vectors encoding full-length RIP1 or FADD and increasing amounts of plasmid encoding Tax. Thirty-six hours later, the cells were subjected to luciferase reporter assay. Error bars, ±SD.

HA-tagged RIP1 into 293T cells along with FLAG-tagged versions of RIG-I or MDA-5. These coimmunoprecipitation experiments indicated that while RIP1 was able to weakly associate with full-length RIG-I and MDA-5, it bound with significantly greater affinity to the CARDs of RIG-I and MDA-5 (Fig. 4B). Taken together, these results suggest that RIP1 may be recruited to RIG-I- and MDA-5-containing complexes upon activation by viral RNA. These findings were confirmed using a yeast two-hybrid assay approach, which indicated a robust association of RIP1 and FADD (His-Leu-Trp-Ade [HLTA]-deficient media) and a weaker association of RIP1 with the CARDs of both RIG-I and MDA5 (HLT-deficient media) (Fig. 4C).

To extend these studies, we cotransfected 293T cells with various domains of RIP1 in the presence of the CARDs of RIG-I or MDA5. This study again indicated that the ID domain of RIP1 associated with the CARD of RIG-I (Fig. 4D). Of interest was that while both Tax and the CARD of RIG-I bound to the ID of RIP1, Tax did not inhibit RIG-I/RIP1 interactions, indicating that TAX and RIG-I bind to different regions of the ID (Fig. 4E).

Significantly, further analysis indicated that RIP1 was able to potently synergize with the CARDS of both RIG-I and MDA5 to induce activation of the type I IFN promoter (Fig. 4F). A similar approach indicated that the RIP1 ID regions alone were able to manifest the observed synergy with the CARDS of RIG-I and MDA5 (Fig. 4F). A similar effect was observed with FADD (Fig. 4G). However, the presence of Tax was able to block the synergistic effects of RIP1 or FADD with RIG-I, which would otherwise augment the induction of the type I IFN promoter (Fig. 4H and I). Our data thus indicate that the CARDs of RIG-I associate with RIP1, which in turn associates with FADD to facilitate the activation of the type I IFN promoter. Tax association with RIP1 is able to prevent the induction of this pathway.

Tax prevents RIP1 innateosome activation of IRF7. Our data indicate that Tax binds to the ID domain of RIP1 to prevent downstream NF-κB-independent innate immune signaling processes. We therefore investigated whether Tax prevented RIP1 binding to required signaling partners to disrupt innateosome complex formation. Principally, while coimmunoprecipitation analysis indicated that Tax could bind to RIP1, we did not see any appreciable Tax binding to downstream type I IFN signaling components such as TRAF3 or TANK (Fig. 5A and B). Neither did Tax prevent complex association with RIP1 or TBK1 (Fig. 5C). Moreover, Tax did not appear to inhibit TBK-1's association with IRF3 or IRF7 (Fig. 5D and E). Indeed, Tax seemed to slightly enhance the association of some of these innate signaling components, such as TRAF3, perhaps to augment NF-κB activity. However, we confirmed that RIP1 bound efficiently to available IRF7, as has been shown previously (50) (Fig. 5F), but not IRF3. This association was noted to involve IRF7 binding to the ID of RIP1, similar to Tax (Fig. 3F and 5G). Tax did not appear to influence IRF3 activity, as emphasized by analyzing IRF3 dimerization and translocation (Fig. 5H). However, Tax did impede IRF7 function as shown by GAL4-IRF7 assays (Fig. 5I). Given that Tax could bind to RIP1 via the ID, we therefore investigated whether Tax could block RIP1/IRF7 association. Indeed, this coimmunoprecipitation analysis confirmed that Tax could in fact repress RIP1/IRF7 interactions, an effect that likely explained the repressed IRF7 activity (Fig. 5J). Analysis of HTLV-1-transformed C8166 cells, which express endogenous Tax, further confirmed that Tax can indeed inhibit RIP1/IRF7 interactions likely by preferentially associating with RIP1 rather than IRF7 (Fig. 3 and 5K).

Our data also indicate that the CARDs of RIG-I as well as IRF7 associate with the ID of RIP-1, a region that exhibits constitutive activity (Fig. 1D and 5G). Results further show that Tax can block IRF7 association with RIP1 and IRF7 activity (Fig. 5I to K). However, Tax did not robustly inhibit RIG-I binding to RIP1 (Fig. 4E). To examine the molecular mechanisms in more detail, we examined which regions of the RIP1 ID associated with Tax, RIG-I or IRF7. The ID (aa 301 to 558) or portions of the ID (aa 291 to 490 [ID12] or aa 391 to 582 [ID23]) were cloned into expression vectors (Fig. 6A). We principally noted that ID23 alone but not ID12 exerted the ability to stimulate the production of type I IFN (similar to the ID), events that were suppressed in the presence of Tax (Fig. 6B). We noted that IRF7 did not strongly bind to ID12 or 23, perhaps due to the fact that both regions were required for stabilizing the interaction (Fig. 6C). However, we observed that ID12 was not expressed robustly. In contrast, we did observe that Tax strongly interacted with ID23 (aa 391 to 582) (Fig. 6D). The CARDs of RIG-I were similarly found to associate with ID23 (Fig. 6E) but did not appear to inhibit RIP1/RIG-I interactions, suggesting that Tax may bind to a different portion of ID23. To determine this, we created a RIP1 deletion variant lacking aa 391 to 490 (dID2, aa 391 to 490) (Fig. 6F). This construct was developed since generating smaller portions of ID23 resulted in poor expression. Our analysis indicated that Tax did not bind robustly to dID2 in contrast to RIG-1, which exhibited evident binding (Fig. 6G). We thus conclude that IRF7 may bind to the region of aa 301 to 588 of RIP1 and Tax to the region of aa 391 to 490 while RIG-1 associates with a region representing aa 491 to 588 (Fig. 6H). This association is presumably sufficient to prevent RIP1 binding to IRF7, which eliminates IRF7 activity and type I IFN induction. IRF7 is required for the robust activation of predominantly the type I IFN alpha genes rather than the beta interferon gene, which principally uses IRF3 to initiate its transcription after infection of the cell (51). This is because IRF7 is itself type I IFN inducible and not robustly expressed in uninfected cells. Following induction, IRF7 facilitates further IFN-β induction, with IRF3, while robustly stimulating alpha interferon production in a positive-feedback manner. Analysis of poly(I·C)-treated or RNA virus-infected wild-type (WT) or RIP1-deficient MEFs confirmed a more significant requirement for IRF7 in IFN-α induction than in IFN-β induction (Fig. 7A to C). Since IRF7 is the "master regulator" of type I IFN induction, our data indicate that Tax suppression of this activity potently inhibits RIG-I- and TRIF-dependent signaling (52).

DISCUSSION

HTLV-1 is a delta-type retrovirus currently responsible for 10 to 20 million infections worldwide (24). In contrast to the other important human retroviral pathogen, HIV, which proliferates by direct production of progeny virions, HTLV-1 increases its copy number primarily by inducing the proliferation of infected cells (51). Thus, promotion of immortalization and transformation of the infected cell thus appears to be a primary step in viral propagation (53). Leukemogenesis of ATL has been suggested to be a multievent process involving both the disabling of cellular tumor suppressor and apoptotic processes and the engagement of proliferative and antiapoptotic signaling (54). Tax has been reported to be involved in all these events and possesses an essential role in

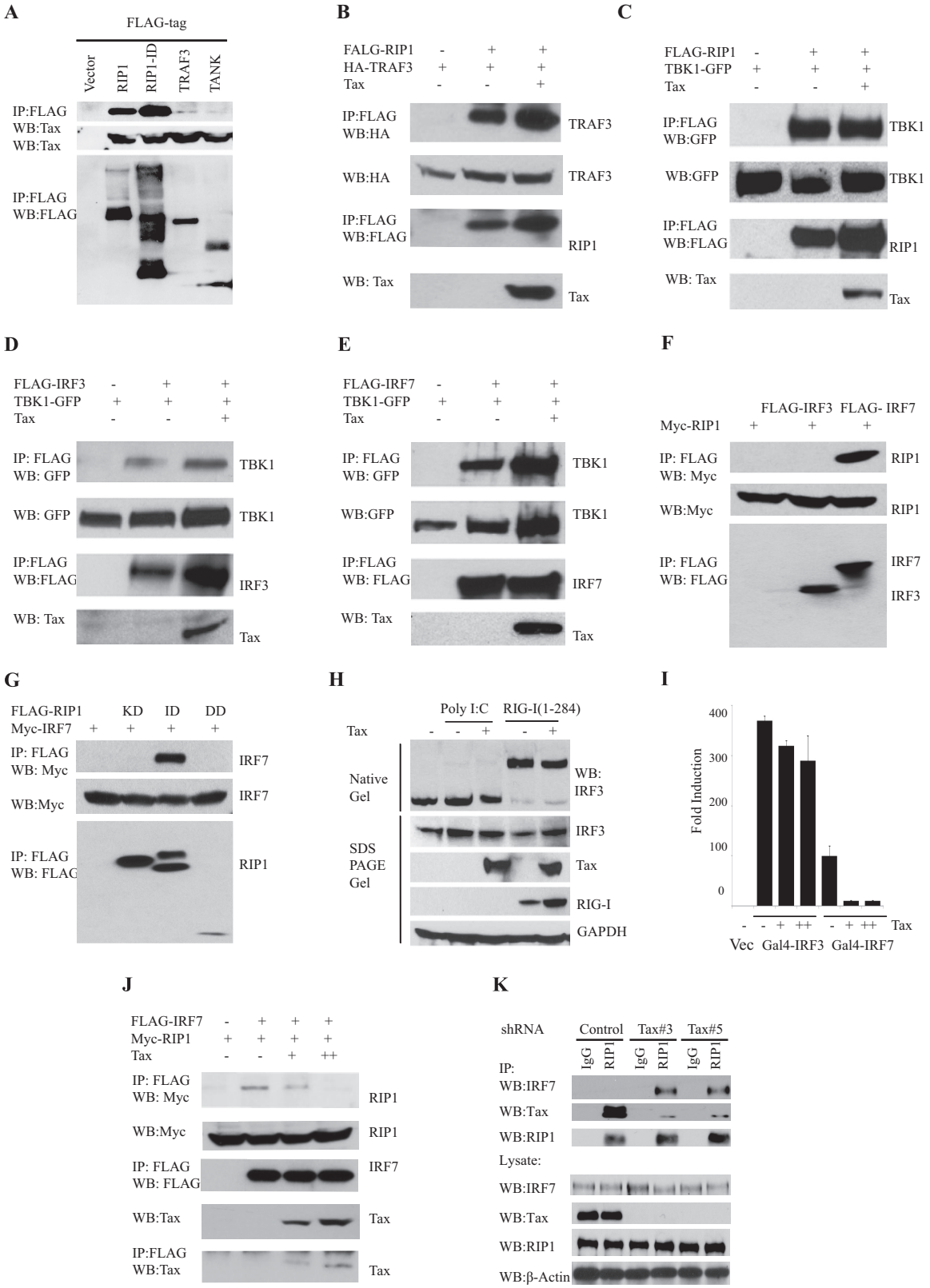

FIG 5 Tax abrogates RIP1 and IRF7 interaction. (A) Co-IP analyses were performed in 293T cells after overexpressing Tax and FLAG-RIP1, FLAG-intermediate domain of RIP1 (aa 301 to 588), FLAG-TRAF3, or FLAG-TANK, using anti-FLAG antibody. IB analyses were done with the indicated antibody. (B) Co-IP analysis was done in 293T cells using expression plasmids encoding FLAG-RIP1 or HA-TRAF3 and either with or without Tax. (C) Co-IP analyses were performed as described for panel A using expression vectors encoding FLAG-RIP1, TBK-GFP, and Tax. (D, E) Co-IP analyses were performed as described for panel A using expression vectors encoding FLAG-IRF3 or FLAG-IRF7, TBK-GFP, and Tax. (F) Co-IP analyses were done in 293T cells as described for panel A

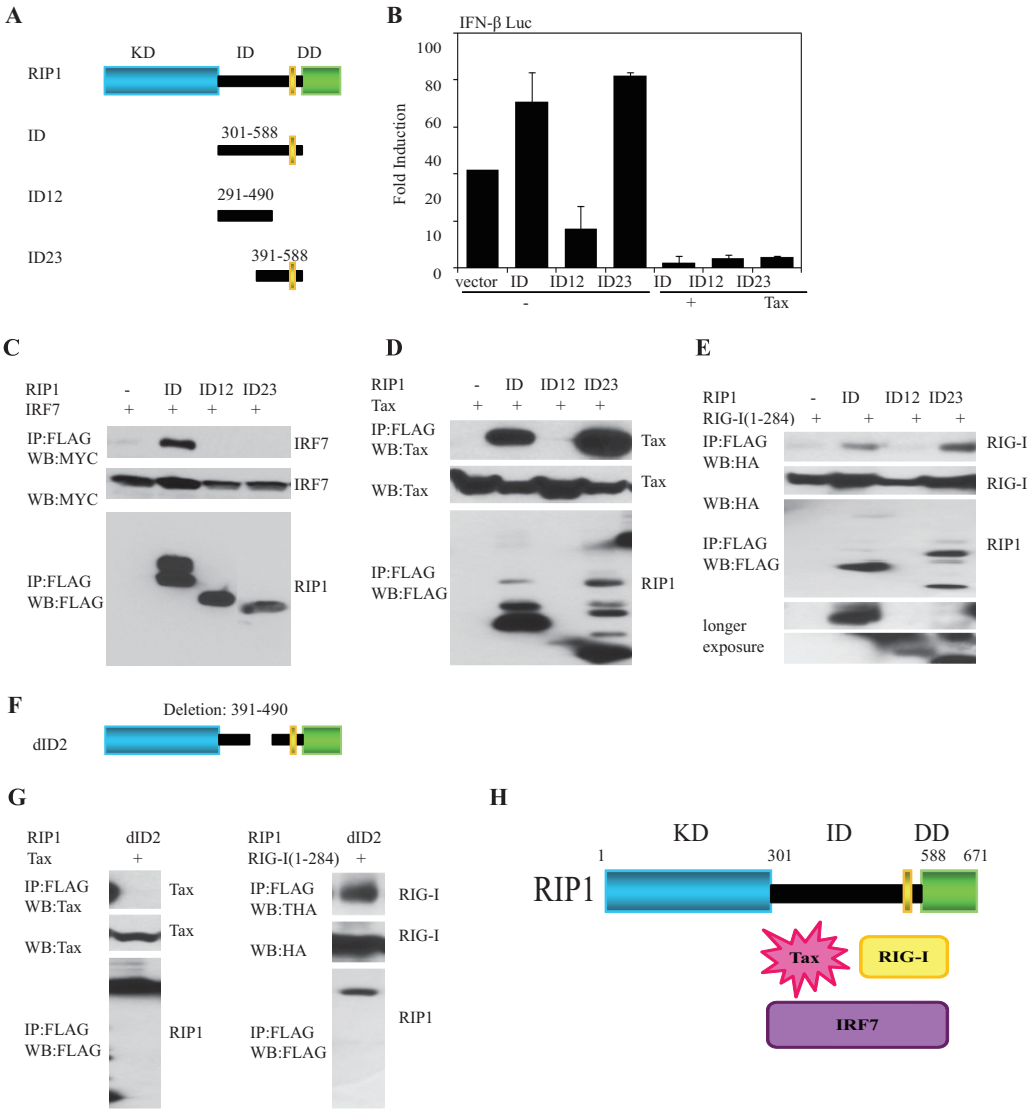

FIG 6 Tax preferentially inhibits activity of IRF7. (A, B) Schematic figures of intermediate domain of RIP1 variants (A) and IFN-β-Luc (B) reporter assays examined in 293T cells using expression vector encoding FLAG-RIG-I(1-284), FLAG-RIP1 (ID, aa 301 to 588), FLAG RIP1(ID12, aa 291 to 490), or FLAG-RIP1(ID23, aa 391 to 588), either with or without Tax. (C, D, E) Co-IP analysis in 293T cells after expressing FLAG-RIP1 (ID, aa 301 to 588), FLAG-RIP1 (ID12, aa 291 to 490), or FLAG-RIP1(ID23, aa 391 to 588), and either Myc-IRF7, Tax, or HA-RIG-I (aa 1 to 284). Thirty-six hours later, cell lysates were immunoprecipitated, and IB analysis was performed with the indicated antibodies. (F) Structure of dID2 (deletion, aa 391 to 490) of RIP1. (G) Co-IP assay revealed that intermediate domain aa 391 to 490 of RIP1 was essential for Tax association to RIP1 but not for HA-RIG-I(1-284). 293T cells were transfected with ID2 of FLAG-RIP1 (deletion, aa 391 to 490), and either Tax or HA-RIG-I(1-284) for 36 h. The lysates were pulled down with anti-FLAG antibody, and IB was performed with anti-Tax antibody. (H) Schematic model of RIP1-interacting proteins and Tax. Error bars, ±SD.

ATL pathogenesis (55). In addition to modifying cellular growth signals to provide proliferative advantages to infected cells, effective counteraction of host immune responses is also essential for successful infection and viral spread. Indeed, in later stages of leukemogenesis, silencing of Tax expression appears to be advantageous for cells capable of maintaining a transformed phenotype without Tax, because Tax is a target of the host acquired immune system. In addition to acquired immune responses to HTLV-1

using plasmids encoding Myc-RIP1 and FLAG-IRF3 or FLAG-IRF7. (G) Co-IP analysis in 293T cells as described for panel A using plasmids encoding full-length Myc-IRF7 and FLAG-RIP1 mutants: kinase domain (aa 1 to 300), intermediate domain (aa 301 to 588), or death domain (aa 589 to 671). (H) Native PAGE gel analysis for IRF3 dimerization in 293T cells with transfection of an empty vector or expression vector encoding HA-RIG-I (aa 1 to 284), either with or without plasmid encoding Tax. The cells were stimulated with poly(I·C) (1 μg/ml) for 4 h, and the lysates were subjected to IB with the indicated antibodies. (I) Luciferase reporter assays were performed in 293T cells after transfecting with GAL4 binding luciferase plasmid and an expression vector encoding GAL4-conjugated full-length IRF3 and full-length IRF7 with increasing amounts of Tax. (J) Co-IP analysis in 293T cells after overexpressing plasmids encoding Myc-RIP1 and FLAG-IRF7 with an increasing amount of Tax. IB analysis was done with the indicated antibodies. (K) Depletion of Tax with shRNAs restores RIP1-IRF7 interaction in HTLV-1-transformed cells. Co-IP analysis was done in C8166 cells after lentiviral transduction of control or Tax short hairpin RNAS (shRNAs) (Tax#3 and Tax#5) for 5 days. IB was performed after IgG control or RIP1 IP with the indicated antibodies. Error bars, ±SD.

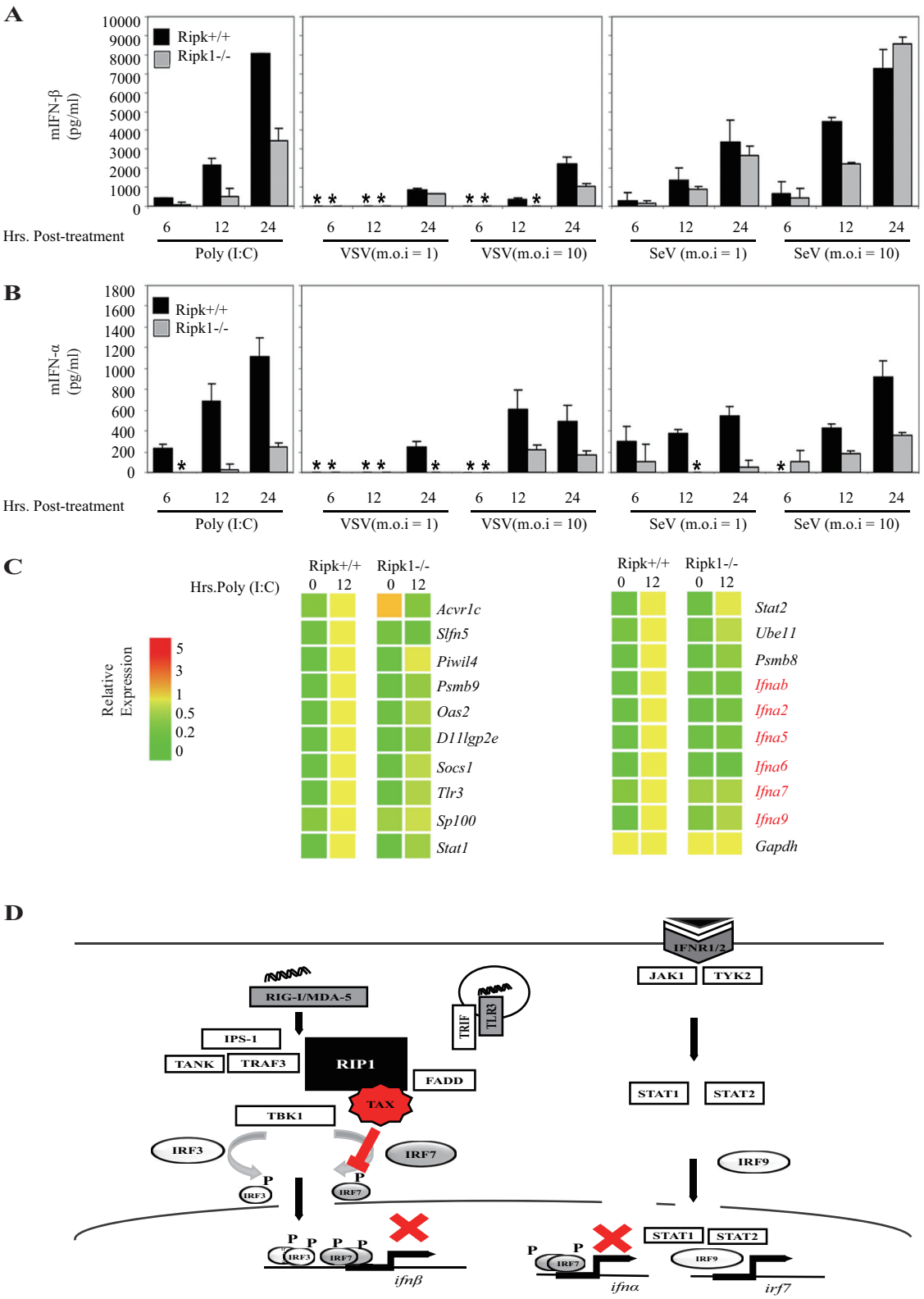

FIG 7 RIP1 is involved in the induction of IFN-α. (A, B) ELISA measurements of IFN-β and IFN-α with supernatants of RIP1$^{+/+}$ and RIP1$^{-/-}$ MEFs after stimulation with poly(I·C), VSV, or SeV at MOIs of 1 and 10. Error bars, SD. (C) Microarray analysis of dsRNA-inducible genes were performed in RIP1$^{+/+}$ and RIP1$^{-/-}$ MEFs after treatment with poly(I·C) for 12 h. (D) A model of Tax suppression of innate immune signaling. RNA sensor RIG-I, MDA-5, or TLR3 recognizes and activates IPS-1 or TRIF, forming a complex with molecules TRAF3, FADD, and RIP1. This leads to phosphorylation of TBK1, which phosphorylates the transcription factor IRF3 for primary IFN-β induction. Secreted IFN-β binds to IFN receptors and induces *ifn* α and *irf7* through JAK/STAT signaling. HTLV-1 viral protein Tax strongly binds to RIP1 to impede IRF7 function and type I IFN signaling.

infection, however, powerful innate mechanisms that recognize and limit viral replication exist.

Here, we show that HTLV-1 Tax potently inhibits antiviral signaling by one of these important mechanisms. Signaling by the RNA helicases RIG-I and MDA-5 has recently emerged as pivotal for the production of type I IFNs in response to cytosolic viral RNA species (10, 11). Although the exact signaling events downstream of RIG-I and MDA-5 remain unclear, it appears that IPS-1, TRAF3, FADD, and RIP1 participate in the activation of IRF3/7 (13, 17, 18, 43). In this study, we demonstrate that HTLV-1 Tax inhibits the production of type I IFN by the RNA helicases RIG-I and MDA-5. Tax was found to interact with RIP1, a kinase previously shown by our group and others to possess a role in the production of type I IFN and protection against virus infection. We further show that RIP1 associates with the CARDs of RIG-I and MDA-5 and confirm its essential role in signaling downstream of these helicases. Specifically, we show that RIP1 is indispensable for the robust production of IFN-α and other secondary genes after dsRNA stimulation of virus infection. RIP1 interacted with the CARDs of RIG-I and MDA-5 via its ID. Overexpression of RIP1 synergized with the CARDs of RIG-I and MDA-5 to activate IFN, an event which was inhibited by Tax coexpression. TRIF has also been shown to exhibit an RHIM domain and was similarly able to bind to Tax in our studies. TRIF facilitates endosomal TLR3 signaling mediated by dsRNA species. Thus, Tax inhibits TRIF function as well RIG-I/MDA5 and so evades two major antiviral host defense pathways (55).

Following recruitment to RIG-I/MDA5, the molecular events linking RIP1 to the induction of type I IFN genes are somewhat less clear. Recent data show that the transcription factor IRF7 is the "master regulator" of type I IFN production and is essential for IFN-α production (52). In most cell types, IRF7 is a short-lived protein whose levels are controlled by an autocrine loop involving primary IFNs (such as IFN-β and IFN-α4) and whose activation is governed by virus-dependent phosphorylation via cellular TBK-1. Thus, RIP1 and TRIF likely govern IFN-α production via control of IRF7. Our data indicate that this event is prevented by Tax binding to RIP1/TRIF and impeding IRF7 activity.

While our findings suggest Tax binding to RIP1 as a mechanism for inhibition of RIG-I and MDA-5, they do not preclude other mechanisms of innate immune evasion by this key viral oncoprotein. For example, our data indicate that, at higher concentrations, Tax also inhibits activation of type I IFN by activated IRF3/7, presumably by competition for transcription cofactors such as CBP/p300 (56).

Because of their pivotal role in antiviral host defense, innate immune viral recognition pathways are often targeted for inhibition by viruses. For example, the V protein encoded by paramyxoviruses can interact with and inhibit both Mda5 and Stat1 signaling (11). In a growing list of such proteins, data demonstrate that the P protein encoded by Borna disease virus can bind to and inactivate TBK-1, the NS3/4a protease encoded by hepatitis C virus can cleave and disable IPS-1, and the vaccinia virus A52R and N1L proteins interfere with both TLR-dependent and -independent signaling (13, 57, 58). Additionally, our recent findings show that the FADD-interacting poxviral protein MC159 can inhibit RIG-I- and IPS-1-dependent activation of *Ifnb* (42). In summary, our results imply that the suppression of RIP1 facilitated innate immune antiviral signaling as a further important role for Tax in the promotion of leukemogenesis.

ACKNOWLEDGMENTS

We thank H. Ishikawa, N. Shembade, and K. Parvatiyar for technical support and G. Cheng and T. Maniatis for plasmid constructs. We also thank J. Ahn and D. Gutman for assistance with the manuscript submission.

These studies were supported by NIH grant U01AI083015. The content is solely our responsibility and does not necessarily represent the official views of the National Institutes of Health.

REFERENCES

1. **Janeway CA, Jr, Medzhitov R.** 2002. Innate immune recognition. Annu Rev Immunol **20:**197–216. http://dx.doi.org/10.1146/annurev.immunol.20.083001.084359.
2. **Kawai T, Akira S.** 2010. The role of pattern-recognition receptors in innate immunity: update on Toll-like receptors. Nat Immunol **11:**373–384. http://dx.doi.org/10.1038/ni.1863.
3. **Alexopoulou L, Holt AC, Medzhitov R, Flavell RA.** 2001. Recognition of double-stranded RNA and activation of NF-kappaB by Toll-like receptor 3. Nature **413:**732–738. http://dx.doi.org/10.1038/35099560.
4. **Yamamoto M, Sato S, Mori K, Hoshino K, Takeuchi O, Takeda K, Akira S.** 2002. Cutting edge: a novel Toll/IL-1 receptor domain-containing adapter that preferentially activates the IFN-beta promoter in the Toll-like receptor signaling. J Immunol **169:**6668–6672. http://dx.doi.org/10.4049/jimmunol.169.12.6668.
5. **Oshiumi H, Matsumoto M, Funami K, Akazawa T, Seya T.** 2003. TICAM-1, an adaptor molecule that participates in Toll-like receptor 3-mediated interferon-beta induction. Nat Immunol **4:**161–167. http://dx.doi.org/10.1038/ni886.
6. **Yamamoto M, Sato S, Hemmi H, Hoshino K, Kaisho T, Sanjo H, Takeuchi O, Sugiyama M, Okabe M, Takeda K, Akira S.** 2003. Role of adaptor TRIF in the MyD88-independent toll-like receptor signaling pathway. Science **301:**640–643. http://dx.doi.org/10.1126/science.1087262.
7. **Lund JM, Alexopoulou L, Sato A, Karow M, Adams NC, Gale NW, Iwasaki A, Flavell RA.** 2004. Recognition of single-stranded RNA viruses by Toll-like receptor 7. Proc Natl Acad Sci U S A **101:**5598–5603. http://dx.doi.org/10.1073/pnas.0400937101.
8. **Heil F, Hemmi H, Hochrein H, Ampenberger F, Kirschning C, Akira S, Lipford G, Wagner H, Bauer S.** 2004. Species-specific recognition of single-stranded RNA via toll-like receptor 7 and 8. Science **303:**1526–1529. http://dx.doi.org/10.1126/science.1093620.
9. **Diebold SS, Kaisho T, Hemmi H, Akira S, Reis e Sousa C.** 2004. Innate antiviral responses by means of TLR7-mediated recognition of single-stranded RNA. Science **303:**1529–1531. http://dx.doi.org/10.1126/science.1093616.
10. **Yoneyama M, Kikuchi M, Natsukawa T, Shinobu N, Imaizumi T, Miyagishi M, Taira K, Akira S, Fujita T.** 2004. The RNA helicase RIG-I has an essential function in double-stranded RNA-induced innate antiviral responses. Nat Immunol **5:**730–737. http://dx.doi.org/10.1038/ni1087.
11. **Andrejeva J, Childs KS, Young DF, Carlos TS, Stock N, Goodbourn S, Randall RE.** 2004. The V proteins of paramyxoviruses bind the IFN-inducible RNA helicase, mda-5, and inhibit its activation of the IFN-beta promoter. Proc Natl Acad Sci U S A **101:**17264–17269. http://dx.doi.org/10.1073/pnas.0407639101.
12. **Kato H, Takeuchi O, Sato S, Yoneyama M, Yamamoto M, Matsui K, Uematsu S, Jung A, Kawai T, Ishii KJ, Yamaguchi O, Otsu K, Tsujimura T, Koh CS, Reis e Sousa C, Matsuura Y, Fujita T, Akira S.** 2006. Differential roles of MDA5 and RIG-I helicases in the recognition of RNA viruses. Nature **441:**101–105. http://dx.doi.org/10.1038/nature04734.
13. **Kawai T, Takahashi K, Sato S, Coban C, Kumar H, Kato H, Ishii KJ, Takeuchi O, Akira S.** 2005. IPS-1, an adaptor triggering RIG-I- and Mda5-mediated type I interferon induction. Nat Immunol **6:**981–988. http://dx.doi.org/10.1038/ni1243.
14. **Seth RB, Sun L, Ea CK, Chen ZJ.** 2005. Identification and characterization of MAVS, a mitochondrial antiviral signaling protein that activates NF-kappaB and IRF 3. Cell **122:**669–682. http://dx.doi.org/10.1016/j.cell.2005.08.012.
15. **Xu LG, Wang YY, Han KJ, Li LY, Zhai Z, Shu HB.** 2005. VISA is an adapter protein required for virus-triggered IFN-beta signaling. Mol Cell **19:**727–740. http://dx.doi.org/10.1016/j.molcel.2005.08.014.
16. **Meylan E, Curran J, Hofmann K, Moradpour D, Binder M, Bartenschlager R, Tschopp J.** 2005. Cardif is an adaptor protein in the RIG-I

antiviral pathway and is targeted by hepatitis C virus. Nature **437:**1167–1172. http://dx.doi.org/10.1038/nature04193.
17. **Balachandran S, Thomas E, Barber GN.** 2004. A FADD-dependent innate immune mechanism in mammalian cells. Nature **432:**401–405. http://dx.doi.org/10.1038/nature03124.
18. **Oganesyan G, Saha SK, Guo B, He JQ, Shahangian A, Zarnegar B, Perry A, Cheng G.** 2006. Critical role of TRAF3 in the Toll-like receptor-dependent and -independent antiviral response. Nature **439:**208–211. http://dx.doi.org/10.1038/nature04374.
19. **Zhao T, Yang L, Sun Q, Arguello M, Ballard DW, Hiscott J, Lin R.** 2007. The NEMO adaptor bridges the nuclear factor-kappaB and interferon regulatory factor signaling pathways. Nat Immunol **8:**592–600. http://dx.doi.org/10.1038/ni1465.
20. **Watanabe T, Seiki M, Yoshida M.** 1983. Retrovirus terminology. Science **222:**1178.
21. **Poiesz BJ, Ruscetti FW, Gazdar AF, Bunn PA, Minna JD, Gallo RC.** 1980. Detection and isolation of type C retrovirus particles from fresh and cultured lymphocytes of a patient with cutaneous T-cell lymphoma. Proc Natl Acad Sci U S A **77:**7415–7419. http://dx.doi.org/10.1073/pnas.77.12.7415.
22. **Yoshida M, Miyoshi I, Hinuma Y.** 1982. Isolation and characterization of retrovirus from cell lines of human adult T-cell leukemia and its implication in the disease. Proc Natl Acad Sci U S A **79:**2031–2035. http://dx.doi.org/10.1073/pnas.79.6.2031.
23. **Nakayama D, Katamine S, Kanazawa H, Shibuya N, Kawase K, Moriuchi R, Miyamoto T, Hino S.** 1990. Amplification of HTLV-1-related sequences among patients with neurological disorders in highly endemic Nagasaki: lack of evidence for association of HTLV-1 with multiple sclerosis. Jpn J Cancer Res **81:**238–246. http://dx.doi.org/10.1111/j.1349-7006.1990.tb02556.x.
24. **Arisawa K, Soda M, Endo S, Kurokawa K, Katamine S, Shimokawa I, Koba T, Takahashi T, Saito H, Doi H, Shirahama S.** 2000. Evaluation of adult T-cell leukemia/lymphoma incidence and its impact on non-Hodgkin lymphoma incidence in southwestern Japan. Int J Cancer **85:**319–324. http://dx.doi.org/10.1002/(SICI)1097-0215(20000201)85:3<319::AID-IJC4>3.0.CO;2-B.
25. **Akagi T, Ono H, Shimotohno K.** 1995. Characterization of T cells immortalized by Tax1 of human T-cell leukemia virus type 1. Blood **86:**4243–4249.
26. **Tanaka A, Takahashi C, Yamaoka S, Nosaka T, Maki M, Hatanaka M.** 1990. Oncogenic transformation by the tax gene of human T-cell leukemia virus type I in vitro. Proc Natl Acad Sci U S A **87:**1071–1075. http://dx.doi.org/10.1073/pnas.87.3.1071.
27. **Ruben S, Poteat H, Tan TH, Kawakami K, Roeder R, Haseltine W, Rosen CA.** 1988. Cellular transcription factors and regulation of IL-2 receptor gene expression by HTLV-I tax gene product. Science **241:**89–92. http://dx.doi.org/10.1126/science.2838905.
28. **Ballard DW, Bohnlein E, Lowenthal JW, Wano Y, Franza BR, Greene WC.** 1988. HTLV-I tax induces cellular proteins that activate the kappa B element in the IL-2 receptor alpha gene. Science **241:**1652–1655. http://dx.doi.org/10.1126/science.2843985.
29. **Smith MR, Greene WC.** 1990. Identification of HTLV-I tax trans-activator mutants exhibiting novel transcriptional phenotypes. Genes Dev **4:**1875–1885. http://dx.doi.org/10.1101/gad.4.11.1875.
30. **Boxus M, Twizere JC, Legros S, Dewulf JF, Kettmann R, Willems L.** 2008. The HTLV-1 Tax interactome. Retrovirology **5:**76. http://dx.doi.org/10.1186/1742-4690-5-76.
31. **Harhaj EW, Harhaj NS.** 2005. Mechanisms of persistent NF-kappaB activation by HTLV-I tax. IUBMB Life **57:**83–91. http://dx.doi.org/10.1080/15216540500078715.
32. **Grassmann R, Aboud M, Jeang KT.** 2005. Molecular mechanisms of cellular transformation by HTLV-1 Tax. Oncogene **24:**5976–5985. http://dx.doi.org/10.1038/sj.onc.1208978.
33. **Suzuki T, Kitao S, Matsushime H, Yoshida M.** 1996. HTLV-1 Tax protein interacts with cyclin-dependent kinase inhibitor p16INK4A and counteracts its inhibitory activity towards CDK4. EMBO J **15:**1607–1614.
34. **Neuveut C, Low KG, Maldarelli F, Schmitt I, Majone F, Grassmann R, Jeang KT.** 1998. Human T-cell leukemia virus type 1 Tax and cell cycle progression: role of cyclin D-cdk and p110Rb. Mol Cell Biol **18:**3620–3632.
35. **Ishikawa H, Barber GN.** 2008. STING is an endoplasmic reticulum adaptor that facilitates innate immune signalling. Nature **455:**674–678. http://dx.doi.org/10.1038/nature07317.
36. **Ishikawa H, Ma Z, Barber GN.** 2009. STING regulates intracellular DNA-mediated, type I interferon-dependent innate immunity. Nature **461:**788–792. http://dx.doi.org/10.1038/nature08476.
37. **Merrick WC, Kemper WM, Anderson WF.** 1975. Purification and characterization of homogeneous initiation factor M2A from rabbit reticulocytes. J Biol Chem **250:**5556–5562.
38. **Komuro A, Bamming D, Horvath CM.** 2008. Negative regulation of cytoplasmic RNA-mediated antiviral signaling. Cytokine **43:**350–358. http://dx.doi.org/10.1016/j.cyto.2008.07.011.
39. **Belkowski LS, Sen GC.** 1987. Inhibition of vesicular stomatitis viral mRNA synthesis by interferons. J Virol **61:**653–660.
40. **Fontoura BM, Faria PA, Nussenzveig DR.** 2005. Viral interactions with the nuclear transport machinery: discovering and disrupting pathways. IUBMB Life **57:**65–72. http://dx.doi.org/10.1080/15216540500078608.
41. **Panne D.** 2008. The enhanceosome. Curr Opin Struct Biol **18:**236–242. http://dx.doi.org/10.1016/j.sbi.2007.12.002.
42. **Balachandran S, Venkataraman T, Fisher PB, Barber GN.** 2007. Fas-associated death domain-containing protein-mediated antiviral innate immune signaling involves the regulation of Irf7. J Immunol **178:**2429–2439. http://dx.doi.org/10.4049/jimmunol.178.4.2429.
43. **Michallet MC, Meylan E, Ermolaeva MA, Vazquez J, Rebsamen M, Curran J, Poeck H, Bscheider M, Hartmann G, Konig M, Kalinke U, Pasparakis M, Tschopp J.** 2008. TRADD protein is an essential component of the RIG-like helicase antiviral pathway. Immunity **28:**651–661. http://dx.doi.org/10.1016/j.immuni.2008.03.013.
44. **Rajput A, Kovalenko A, Bogdanov K, Yang SH, Kang TB, Kim JC, Du J, Wallach D.** 2011. RIG-I RNA helicase activation of IRF3 transcription factor is negatively regulated by caspase-8-mediated cleavage of the RIP1 protein. Immunity **34:**340–351. http://dx.doi.org/10.1016/j.immuni.2010.12.018.
45. **Feng S, Yang Y, Mei Y, Ma L, Zhu DE, Hoti N, Castanares M, Wu M.** 2007. Cleavage of RIP3 inactivates its caspase-independent apoptosis pathway by removal of kinase domain. Cell Signal **19:**2056–2067. http://dx.doi.org/10.1016/j.cellsig.2007.05.016.
46. **Meylan E, Burns K, Hofmann K, Blancheteau V, Martinon F, Kelliher M, Tschopp J.** 2004. RIP1 is an essential mediator of Toll-like receptor 3-induced NF-kappa B activation. Nat Immunol **5:**503–507. http://dx.doi.org/10.1038/ni1061.
47. **Vandenabeele P, Declercq W, Van Herreweghe F, Vanden Berghe T.** 2010. The role of the kinases RIP1 and RIP3 in TNF-induced necrosis. Sci Signal **3:**re4. http://dx.doi.org/10.1126/scisignal.3115re4.
48. **Cusson-Hermance N, Khurana S, Lee TH, Fitzgerald KA, Kelliher MA.** 2005. Rip1 mediates the Trif-dependent toll-like receptor 3- and 4-induced NF-{kappa}B activation but does not contribute to interferon regulatory factor 3 activation. J Biol Chem **280:**36560–36566. http://dx.doi.org/10.1074/jbc.M506831200.
49. **Hoebe K, Janssen EM, Kim SO, Alexopoulou L, Flavell RA, Han J, Beutler B.** 2003. Upregulation of costimulatory molecules induced by lipopolysaccharide and double-stranded RNA occurs by Trif-dependent and Trif-independent pathways. Nat Immunol **4:**1223–1229. http://dx.doi.org/10.1038/ni1010.
50. **Huye LE, Ning S, Kelliher M, Pagano JS.** 2007. Interferon regulatory factor 7 is activated by a viral oncoprotein through RIP-dependent ubiquitination. Mol Cell Biol **27:**2910–2918. http://dx.doi.org/10.1128/MCB.02256-06.
51. **Matsuoka M.** 2003. Human T-cell leukemia virus type I and adult T-cell leukemia. Oncogene **22:**5131–5140. http://dx.doi.org/10.1038/sj.onc.1206551.
52. **Honda K, Yanai H, Negishi H, Asagiri M, Sato M, Mizutani T, Shimada N, Ohba Y, Takaoka A, Yoshida N, Taniguchi T.** 2005. IRF-7 is the master regulator of type-I interferon-dependent immune responses. Nature **434:**772–777. http://dx.doi.org/10.1038/nature03464.
53. **Igakura T, Stinchcombe JC, Goon PK, Taylor GP, Weber JN, Griffiths GM, Tanaka Y, Osame M, Bangham CR.** 2003. Spread of HTLV-I between lymphocytes by virus-induced polarization of the cytoskeleton. Science **299:**1713–1716. http://dx.doi.org/10.1126/science.1080115.
54. **Matsuoka M, Jeang KT.** 2007. Human T-cell leukaemia virus type 1 (HTLV-1) infectivity and cellular transformation. Nat Rev Cancer **7:**270–280. http://dx.doi.org/10.1038/nrc2111.
55. **Takeda K, Akira S.** 2004. TLR signaling pathways. Semin Immunol **16:**3–9. http://dx.doi.org/10.1016/j.smim.2003.10.003.
56. **Zhang J, Yamada O, Kawagishi K, Araki H, Yamaoka S, Hattori T, Shimotohno K.** 2008. Human T-cell leukemia virus type 1 Tax modulates

interferon-alpha signal transduction through competitive usage of the coactivator CBP/p300. Virology **379:**306–313. http://dx.doi.org/10.1016/j.virol.2008.06.035.

57. **DiPerna G, Stack J, Bowie AG, Boyd A, Kotwal G, Zhang Z, Arvikar S, Latz E, Fitzgerald KA, Marshall WL.** 2004. Poxvirus protein N1L targets the I-kappaB kinase complex, inhibits signaling to NF-kappaB by the tumor necrosis factor superfamily of receptors, and inhibits NF-kappaB and IRF3 signaling by toll-like receptors. J Biol Chem **279:**36570–36578. http://dx.doi.org/10.1074/jbc.M400567200.
58. **Unterstab G, Ludwig S, Anton A, Planz O, Dauber B, Krappmann D, Heins G, Ehrhardt C, Wolff T.** 2005. Viral targeting of the interferon-{beta}-inducing Traf family member-associated NF-{kappa}B activator (TANK)-binding kinase-1. Proc Natl Acad Sci U S A **102:**13640–13645. http://dx.doi.org/10.1073/pnas.0502883102.